Asian Journal of Control, Vol. 17, No. 6, pp. 1–19, November 2015
Published online in Wiley Online Library (wileyonlinelibrary.com) DOI: 10.1002/asjc.1013

MULTIVARIABLE OUTPUT FEEDBACK ADAPTIVE TERMINAL SLIDING MODE CONTROL FOR UNDERWATER VEHICLES

Yaoyao Wang, Linyi Gu, Ming Gao, and Kangwu Zhu

ABSTRACT

For the four degrees of freedom (4-DOF) trajectory tracking control problem of underwater vehicles in the presence of parametric uncertainties and external disturbances, a novel multivariable output feedback adaptive nonsingular terminal sliding mode control (ANTSMC) approach is proposed based on the equivalent output injection adaptive sliding mode observer (ASMO) and ANTSMC method. The ASMO is applied to reconstruct the full states in finite time and the ANTSMC method is designed to stabilize the trajectory tracking error to a small field in finite time. The proposed output feedback ANTSMC approach, using the adaptive technology, does not require the bound information of parametric uncertainties or external disturbances which successfully achieves the decrease of undesired chattering effectively. Corresponding stability analysis is presented. Comparative numerical simulation results are presented to validate the effectiveness of the proposed approach.

Key Words: Output feedback, adaptive sliding mode observer, adaptive nonsingular terminal sliding mode control, equivalent injection, multivariable control.

I. INTRODUCTION

Underwater vehicles, especially remotely operated vehicles (ROVs), have attracted a lot of attention since they are widely applied in military, commercial and scientific investigations. Usually, high accuracy motion and fast dynamic response are required during specific tasks. However, this is a very challenging job due to the notable difficulties in designing the control systems of ROVs. Major difficulties in controlling ROVs include the highly nonlinear time-varying dynamic behavior, uncertainties in hydrodynamic coefficients and disturbances, [1].

Sliding mode control (SMC) is an efficient robust approach to deal with the above-mentioned difficulties. This is mainly due to its attractiveness such as strong robustness, order reduction, easier implementation and design simplification [2]. It has been widely used in many practical systems in the past few decades, such as autonomous underwater vehicles [3], ROVs [4], discrete time-delay singular systems [5], permanent magnet synchronous motor (PMSM) drives [6], and launch vehicles [7]. Usually, conventional SMC is linear hyperplane-based, which means the control system can only achieve asymptotic stability and the trajectory tracking errors cannot converge to zero in finite time.

It is believed, however, that finite-time stabilization of dynamical systems may give rise to higher-precision performance and better system dynamic response [8]. Thus, terminal sliding mode control (TSMC) which is a variant scheme of SMC that can achieve finite-time stability, was proposed [9,10]. Inspired by this idea, many researchers had been dedicated to the development of control systems with TSMC. Using a hierarchical TSM structure, finite time reachability of system equilibrium was ensured for multi-input uncertain linear systems, meanwhile existence conditions of TSM and implementability of TSMC were also given [11]. Combining a new non-singularity TSM and a discontinuous reaching law, a non-singular TSMC was presented to achieve finite time stability for the control of rigid manipulators [12]. Based on a non-singular TSM and a fast TSM-type reaching law, a continuous TSMC was presented [8], which is totally chattering-free, by removing the signum function. Using a time-delay estimation (TDE) algorithm and a non-singular TSM, a practical TSMC for the control of robot manipulator was presented [13]. Combining synchronized control and TSMC, a finite-time approach for formation control of multiple mobile robots with TSM was presented [14]. In light of adaptive robust control (ARC), an adaptive nonsingular fast TSMC was applied to the electromechanical actuator [15]. Using adaptive technology to estimate the

Manuscript received August 16, 2013; revised February 23, 2014; accepted June 12, 2014.

Yaoyao Wang, Linyi Gu (corresponding author, e-mail: lygu@zju.edu.cn) and Ming Gao are with The State Key Laboratory of Fluid Power Transmission and Control, Zhejiang University, Hangzhou 310027, China.

Kangwu Zhu is with Shanghai Institute of Spaceflight Control Technology, Shanghai 200233, China.

This work was supported by Science Fund for Creative Research Groups of National Natural Science Foundation of China (Grant:51221004).

uncertainties, a robust adaptive TSMC was presented for a class of non-autonomous chaotic systems without known bounds of system uncertainties and external disturbances [16]. To summarize the aforementioned works, theoretical studies of TSMC were focused on eliminating singularity and extending to higher order TSMC. Physical applications of TSMC were reported in many areas, like robot manipulators, multi-robot systems, vehicular following system and thrust active magnetic bearing.

Recalling the development of TSMC, almost all the theoretical studies and practical applications were focused on full state feedback TSMC. However, in many applications, full states usually cannot be obtained easily. Hence, a lot of state observers for linear/nonlinear systems had been successfully developed [6,7,17–25]. But most of the observers can only achieve asymptotical stability and require infinite time to estimate the system state in theory. If using these asymptotical state observers, the finite time convergence property of TSMC will be lost [26].

Recently, an output feedback TSMC for a class of second order nonlinear single input and single output (SISO) systems was firstly proposed [26], in which an equivalent output injection sliding mode observer (SMO) was used to estimate the system state. The observer [27,28] can achieve finite-time states estimation and also have good robustness against lumped disturbances. Although exciting results were obtained in [26], it still has two main aspects to be improved. (i) Bound information of lumped uncertainties were still needed which, however, is almost impossible to acquire in many applications. Meanwhile, if bound information cannot be achieved, large feedback gains are required to suppress the lumped uncertainties and ensure the stability of the observer-controller system. This may lead to very serious chattering for both velocity estimation and control effort. (ii) The proposed TSMC approach was specifically designed for SISO systems. Detailed stability analysis and validation were not given for multi input and multi output (MIMO) systems.

In this article the above-mentioned disadvantages are addressed. A multivariable output feedback adaptive nonsingular TSMC (ANTSMC) approach for MIMO control systems of ROVs is proposed. Compared with [26] and [27], the new proposed approach is much more challenging in system analysis and synthesis due to the complexity of the MIMO systems and the application of adaptive control law.

Accordingly, the contribution we try to make is as follows: (i) Synthesize adaptive method with output feedback TSMC for MIMO systems to obtain both finite time stabilization and smooth control effort; (ii) Prove the finite-time convergence of the proposed method with adaptive dynamics and give the velocity estimation and trajectory tracking errors caused by the adoption of adaptive method.

The remainder is organized as follows. In Section II, the modelling of ROVs is given. In Section III, the multivariable output feedback ANTSMC is designed with corresponding stability analysis. In Section IV, comparative simulations are performed to validate the effectiveness of the proposed approach. Finally, some brief conclusions are given in Section V.

II. MODELLING OF REMOTELY OPERATED VEHICLES

The simplified mathematical model of a ROV in four degrees of freedom (4-DOF), described in the earth-fixed coordinate frame and body-fixed coordinate frame as indicated in Fig. 1, can be expressed as [29]:

$$\begin{aligned} &\dot{\eta} = J(\eta)v \\ &M\dot{v} + C(v)v + D(v)v + g(\eta) = \tau + J^T(\eta)d \\ &\tau = Bu \end{aligned} \tag{1}$$

where $\eta = [x, y, z, \psi]^T$ denotes the ROV's position and orientation in the earth-fixed frame. $v = [u, v, w, r]^T$ is the vector of ROV's linear and angular velocity in the body-fixed frame. $M = M_0 + \Delta M \in \mathbb{R}^{4\times4}$ is the inertial matrix including added mass. $C(v) = C_0(v) + \Delta C(v) \in \mathbb{R}^{4\times4}$ is the Coriolis and centripetal forces. $D(v) = D_0(v) + \Delta D(v) \in \mathbb{R}^{4\times4}$ denotes the hydrodynamic damping term. The vector $g(\eta) = g_0(\eta) + \Delta g(\eta) \in \mathbb{R}^{4\times1}$ is a combined force/moment of gravity and buoyancy. $M_0, C_0(v), D_0(v), g_0(\eta)$ are the nominal parameter matrices and $\Delta M, \Delta C(v), \Delta D(v), \Delta g(\eta)$ are the parameter uncertainties. $\tau \in \mathbb{R}^{4\times1}$ is the system control effort. $B \in \mathbb{R}^{4\times5}$, the dynamic distribution matrix, is decided

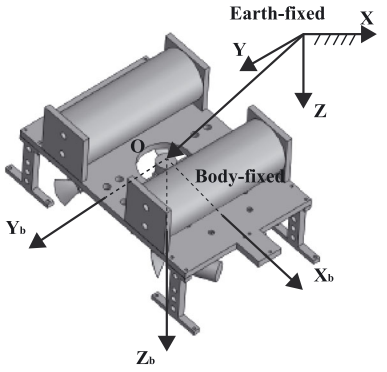

Fig. 1. Earth-fixed and body-fixed frame.

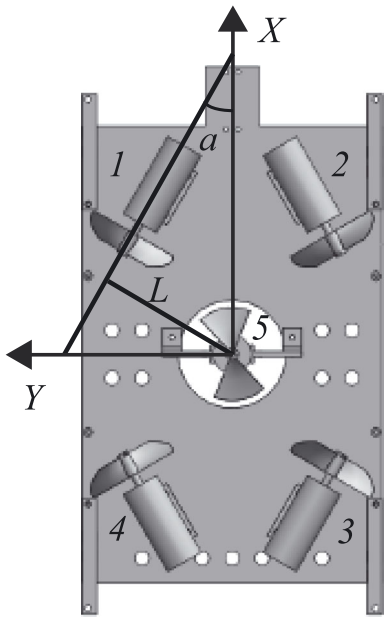

Fig. 2. Arrangement of ROVs' thrusters.

by the arrangement of the ROV's thrusters as indicated in Fig. 2. $u \in \mathbb{R}^{5\times1}$ is the force vector produced by the ROV's thrusters. $d \in \mathbb{R}^{4\times1}$ denotes the external disturbances vector. $J(\eta)$, the kinematic transformation matrix which expresses the transformation from the body-fixed frame to earth-fixed frame, can be described as:

$$J(\eta) = \begin{bmatrix} \cos\psi & -\sin\psi & 0 & 0 \\ \sin\psi & \cos\psi & 0 & 0 \\ 0 & 0 & 1 & 0 \\ 0 & 0 & 0 & 1 \end{bmatrix} \tag{2}$$

The other simplified nominal parameter matrices can be expressed as follows:

$$M_0 = diag\left\{m - X_{\dot{u}}, m - Y_{\dot{v}}, m - Z_{\dot{w}}, I_Z - N_{\dot{r}}\right\} \tag{3}$$

$$C_0(v) = \begin{bmatrix} 0 & 0 & 0 & -\vec{M}_1 v \\ 0 & 0 & 0 & -\vec{M}_2 u \\ 0 & 0 & 0 & 0 \\ \vec{M}_1 v & -\vec{M}_2 u & 0 & 0 \end{bmatrix} \tag{4}$$

$$\begin{aligned} D_0(v) = diag\{&X_u + X_{u|u|}u,\ Y_v + Y_{v|v|}v, \\ &Z_w + Z_{w|w|}w,\ N_r + N_{r|r|}r\} \end{aligned} \tag{5}$$

$$g_0(\eta) = [0, 0, W_B - W, 0]^T \tag{6}$$

$$B = \begin{bmatrix} \cos a & \cos a & -\cos a & -\cos a & 0 \\ -\sin a & \sin a & \sin a & -\sin a & 0 \\ 0 & 0 & 0 & 0 & 1 \\ -L & L & -L & L & 0 \end{bmatrix} \tag{7}$$

where $\vec{M}_1 = m - Y_{\dot{v}}, \vec{M}_2 = m - X_{\dot{u}}$. W_B, W denotes the buoyancy and weight of the ROV's body, and $a = 30°, L = 0.1$m.

III. MULTIVARIABLE OUTPUT FEEDBACK ADAPTIVE NONSINGULAR TERMINAL SLIDING MODE CONTROL

Some preliminaries are given before designing the controller [26,27,30].

Assumption 1. MIMO dynamic system (1) does not have a finite escape time.

Assumption 2. The control input τ belongs to the extended L_p space, denoted as $\tilde{L}_p$ in this work. Any truncation of τ to a finite time interval is bounded.

Assumption 3. The desired trajectory η_d is smooth, *i.e.*, $\dot{\eta}_d, \ddot{\eta}_d$ are bounded and exist.

Definition 1. Consider the nonlinear system $\dot{x} = f(x, u)$, where x is the state vector and u is the input vector. The solution is practical finite-time stable (PFS) if for all $x(t_0) = x_0$, there exist $\delta > 0$ and $T(\delta, x_0) < \infty$, such that $\|x(t)\| < \delta$, for all $t \geq t_0 + T$.

Lemma 1. For any three real numbers a, b, c, if $a + b = c$, then for any positive scalar $h \geq 0.5$, the following inequality holds:

$$ab \leq -\frac{2h-1}{2h}a^2 + \frac{h}{2}c^2 \tag{8}$$

Lemma 2. For any real numbers $x_i, i = 1, \cdots n$ and $0 < b \leq 1$, then the following inequality holds:

$$\left(|x_1| + \cdots + |x_n|\right)^b \leq |x_1|^b + \cdots |x_n|^b \tag{9}$$

Lemma 3. Consider the system $\dot{x} = f(x, u)$. Suppose that there exist continuous function $V(x)$, scales $\lambda > 0, 0 < \mu < 1$ and $0 < \omega < \infty$ such that

$$\dot{V(x)} \leq -\lambda V^{\mu}(x) + \omega \tag{10}$$

Then, the system $\dot{x} = f(x, u)$ is PFS, and the trajectory of the closed-loop system is bounded in finite time as:

$$\lim_{\theta\to\theta_0} x \in \left(V^{\mu}(x) \leq \frac{\omega}{(1-\theta)\lambda}\right) \tag{11}$$

where $0 < \theta_0 < 1$. The time needed to reach the area (11) is bounded as:

$$T \leq \frac{V^{1-\mu}(x_0)}{\lambda\theta_0(1-\mu)} \tag{12}$$

where $V(x_0)$ is the initial value of $V(x)$.

3.1 Multivariable equivalent output injection adaptive SMO design

For simplicity, the following notations will be used: x_i represents the ith component of the vector x, $\hat{x}$ represents the estimation of x. The operation $<, >, \leq, \geq$ for two vector is performed in terms of corresponding elements. $sig(x)^a = \left[|x_1|^{a_1}\text{sgn}(x_1), \cdots, |x_4|^{a_4}\text{sgn}(x_4)\right]^T$.

To simplify design procedure, the nonlinear model of the ROVs in the earth-fixed frame is used [29].

$$\begin{aligned} \dot{\eta} &= v_e = J(\eta)v \\ \overline{M(\eta)}\dot{v}_e + \overline{C(v,\eta)}v_e + \overline{D(v,\eta)}v_e &\\ + \overline{g(\eta)} &= J^{-T}(\eta)\tau + d \end{aligned} \tag{13}$$

where v_e represents the velocity vector in earth-fixed frame of the ROV, and the parameter matrixes in (13) can be described as:

$$\begin{aligned} \overline{M(\eta)} &= J^{-T}(\eta)MJ^{-1}(\eta) \\ \overline{C(v,\eta)} &= J^{-T}\left[C(v) - MJ^{-1}(\eta)\dot{J(\eta)}\right]J^{-1}(\eta) \\ \overline{D(v,\eta)} &= J^{-T}(\eta)D(v)J^{-1}(\eta) \\ \overline{g(\eta)} &= J^{-T}(\eta)g(\eta) \end{aligned}$$

Property 1. The parameter matrices have some great properties in the earth-fixed frame when $M = M^T$ and $\dot{M} = 0$:

$$\begin{aligned} &\overline{M(\eta)} = \overline{M^T(\eta)} > 0, \forall\eta \in \mathbb{R}^{4\times1} \\ &x^T\left[\dot{\overline{M(\eta)}} - 2\overline{C(v,\eta)}\right]x = 0, \forall x, v, \eta \in \mathbb{R}^{4\times1} \\ &\overline{D(v,\eta)} > 0, \forall v, \eta \in \mathbb{R}^{4\times1} \end{aligned}$$

Define $x_1 = \eta \in \mathbb{R}^{4\times1}, x_2 = v_e \in \mathbb{R}^{4\times1}$, then the model of ROVs in the earth-fixed frame is:

$$\begin{aligned} \dot{x}_1 &= x_2 \\ \overline{M_0(x_1)}\dot{x}_2 &= -\overline{C_0(x_1,x_2)}x_2 - \overline{D_0(x_1,x_2)}x_2 \\ &\quad - \overline{g_0(x_1)} + J^{-T}(x_1)\tau + \tau_d \end{aligned} \tag{14}$$

where $\tau_d = d - \overline{\Delta M}\dot{x}_2 - \overline{\Delta C}x_2 - \overline{\Delta D}x_2 - \overline{\Delta g}$.

Assumption 4. The lumped uncertain term $\tau_d(t,x)$ is bounded all the time with a constant unknown vector:

$$|\tau_d| < \xi \in \mathbb{R}^{4\times1} \tag{15}$$

Remark 1. The boundedness of $\tau_d(t,x)$ is essential due to the fact that the force produced by the propellers is doubtlessly bounded. Meanwhile, as $\tau_d(t,x)$ is associated with x_1 and x_2, corresponding stability results given later will be limited to local ones under Assumption 4.

Illumined by [26–28], the following equivalent output injection adaptive SMO (ASMO) for the MIMO systems of ROVs can be designed as:

$$\begin{aligned} \dot{\hat{x}}_1 &= \hat{x}_2 + \gamma_1\text{sgn}\left(\tilde{x}_1\right) \\ \overline{M_0(x_1)}\dot{\hat{x}}_2 &= -\overline{C_0\left(x_1,\hat{x}_2\right)}\hat{x}_2 - \overline{D_0\left(x_1,\hat{x}_2\right)}\hat{x}_2 \\ &\quad - \overline{g_0(x_1)} + J^{-T}(x_1)\tau + \hat{\gamma}_2\text{sgn}\left(\bar{x}_2 - \hat{x}_2\right) \\ \dot{\hat{\gamma}}_2 &= p_0\left(-\varepsilon_0\hat{\gamma}_2 + \left|\bar{x}_2 - \hat{x}_2\right|\right) \end{aligned} \tag{16}$$

where $\tilde{x}_1 = x_1 - \hat{x}_1, \tilde{x}_2 = x_2 - \hat{x}_2$ are the estimation errors. $\gamma_1, \hat{\gamma}_2 \in \mathbb{R}^{4\times1}, p_0 = diag(p_{01}, \ldots, p_{04})$, $\varepsilon_0 = diag(\varepsilon_{01}, \ldots, \varepsilon_{04})$ are positive gain vectors/matrices to be designed. $\bar{x}_2 = \hat{x}_2 + \left(\gamma_1\text{sgn}\left(\tilde{x}_1\right)\right)_{eq} \in \mathbb{R}^{4\times1}$, $\left(\gamma_1\text{sgn}\left(\tilde{x}_1\right)\right)_{eq}$ is the equivalent output injection, which can be obtained by passing the signal $\gamma_1\text{sgn}\left(\tilde{x}_1\right)$ through a low pass filter, details can be found in [28].

Thus, the following observer error dynamics can be obtained from (14), (16):

$$\dot{\tilde{x}}_1 = \tilde{x}_2 - \gamma_1\text{sgn}\left(\tilde{x}_1\right) \tag{17}$$

$$\overline{M_0(x_1)}\dot{\tilde{x}}_2 = -\hat{\gamma}_2\text{sgn}\left(\bar{x}_2 - \hat{x}_2\right) + \tau_d + f(\bullet) \tag{18}$$

$$\dot{\hat{\gamma}}_2 = p_0\left(-\varepsilon_0\hat{\gamma}_2 + \left|\bar{x}_2 - \hat{x}_2\right|\right) \tag{19}$$

where:

$$\begin{aligned} f(\bullet) = &\overline{C_0\left(x_1,\hat{x}_2\right)}\hat{x}_2 - \overline{C_0(x_1,x_2)}x_2 \\ &+ \overline{D_0\left(x_1,\hat{x}_2\right)}\hat{x}_2 - \overline{D_0(x_1,x_2)}x_2. \end{aligned}$$

Theorem 1. Under Assumptions 1–4, the equivalent output injection ASMO (16) for ROVs can guarantee that the estimation error $\tilde{x}_1$ converges to 0 in finite time and $\tilde{x}_2$ converges to the following field in finite time:

$$\left|\tilde{x}_{2i}\right| \leq \Delta_i = \left(\frac{\varepsilon_{0i}h_i\gamma_{2i}^2}{2\varepsilon_{2i}(1-\theta_{0i})}\right) \tag{20}$$

where $h_i \geq 0.5, \varepsilon_{2i} > 0, 0 < \theta_{0i} < 1$. γ_{2i} is the bound of the uncertainties which will be given in the proof.

Proof. The proof will be given in two steps. The first step is similar to the proof presented in [26,27] with the exception that different dynamic equations are used, and the second step uses some tricks from [30].

Step 1. This step will prove that the estimation error $\tilde{x}_1$ will converge to zero in finite time. For simplicity, choose the ith component of the MIMO systems to analyze. Choose a Lyapunov function candidate for the estimation error dynamic equation (17) as:

$$V_{1i} = \frac{1}{2}\tilde{x}_{1i}^2 \tag{21}$$

Differentiating V_{1i} with respect to time along (17) yields:

$$\dot{V}_{1i} = -\gamma_{1i}\left|\tilde{x}_{1i}\right| + \tilde{x}_{1i}\tilde{x}_{2i} \le -\left|\tilde{x}_{1i}\right|\left[\gamma_{1i} - \left|\tilde{x}_{2i}\right|\right] \tag{22}$$

According to Assumptions (1), (2) and (4), the estimation error $\tilde{x}_{2i}$ does not have finite escape time. This guarantees the estimation error $\tilde{x}_{2i}$ within $\tilde{L}_p$ space effectively. Thus, we can choose $\gamma_{1i} > \left|\tilde{x}_{2i}\right| + \varepsilon_{1i}, \varepsilon_{1i} > 0$, which yields:

$$\dot{V}_{1i} \le -\varepsilon_{1i}\left|\tilde{x}_{1i}\right| \tag{23}$$

Hence, finite time convergence of $\tilde{x}_{1i}$ to 0 can be ensured. To satisfy (23) arbitrarily, choose $\gamma_{1i} > \max_{t\in[0,\tilde{T}]}\left|\tilde{x}_{2i}\right|$, where $\tilde{T}$ is chosen large enough such that $\gamma_{1i} > \left|\tilde{x}_{2i}\right| + \varepsilon_{1i}$. Then, we have:

$$\dot{V}_{1i} \le -\varepsilon_{1i}\left|\tilde{x}_{1i}\right| = -\sqrt{2}\varepsilon_{1i}V_{1i}^{0.5} \tag{24}$$

Then, according to the differential inequality principle [31,32], when $t_{1i} \ge t_{0i} + \left|\tilde{x}_{1i}(t_0)\right|/\varepsilon_{1i}$, where t_{0i} is the initial time, $\tilde{x}_{1i} = 0$. Thus, $\tilde{x}_{1i} = \dot{\tilde{x}}_{1i} = 0$ and $\tilde{x}_{2i} = \left(\gamma_{1i}\mathrm{sgn}\left(\tilde{x}_{1i}\right)\right)_{eq}$ on the sliding mode. Therefore, $\mathrm{sgn}\left(\tilde{x}_2 - \hat{x}_2\right)_i = \mathrm{sgn}\left(\tilde{x}_2\right)_i$. Then the estimation error dynamic equations (17)–(18) can be rewritten as:

$$\dot{\tilde{x}}_1 = 0 \tag{25}$$

$$\overline{M_0(x_1)}\dot{\tilde{x}}_2 = -\hat{\gamma}_2\mathrm{sgn}\left(\tilde{x}_2\right) + \tau_d + f(\bullet) \tag{26}$$

Step 2. This step will prove that the estimation error $\tilde{x}_2$ will converge to a small ball field Δ in finite time. Choose a Lyapunov candidate V_{2i} as:

$$V_{2i} = \frac{1}{2}\left(\tilde{x}_{1i}^2 + \overline{M_{0i}}\tilde{x}_{2i}^2\right) + \frac{1}{2p_{0i}}\tilde{\gamma}_{2i}^2 \tag{27}$$

where $\tilde{\gamma}_{2i} = \gamma_{2i} - \hat{\gamma}_{2i}$. γ_{2i} is a constant which will be given later. Since $\tilde{x}_{1i} = 0$ when $t \ge t_{1i}$, thus taking the derivative of V_{2i} along (25)(26) yields:

$$\begin{aligned}\dot{V}_{2i} &= \left(-\hat{\gamma}_2\mathrm{sgn}\left(\tilde{x}_2\right) + \tau_d + f(\bullet)\right)_i\tilde{x}_{2i} \\ &\quad - \tilde{\gamma}_{2i}\left(-\varepsilon_0\hat{\gamma}_2 + \left|\tilde{x}_2\right|\right)_i \\ &\le -\left|\tilde{x}_{2i}\right|\left(\gamma_{2i} - \left|\tau_d + f(\bullet)\right|_i\right) + \varepsilon_{0i}\tilde{\gamma}_{2i}\hat{\gamma}_{2i}\end{aligned} \tag{28}$$

Choosing $\gamma_{2i} > \left|\tau_d + f(\bullet)\right|_i + \varepsilon_{2i}, \varepsilon_{2i} > 0$ yields:

$$\dot{V}_{2i} \le -\varepsilon_{2i}\left|\tilde{x}_{2i}\right| + \varepsilon_{0i}\tilde{\gamma}_{2i}\hat{\gamma}_{2i} \tag{29}$$

Noticing $\tilde{x}_{1i} = 0$ when $t \ge t_1$, then the inequality (29) can be rewritten as:

$$\begin{aligned}\dot{V}_{2i} &\le -\varepsilon_{2i}\left|\tilde{x}_{2i}\right| + \varepsilon_{0i}\tilde{\gamma}_{2i}\hat{\gamma}_{2i} \\ &\le -\varepsilon_{2i}\left(\frac{0.5\overline{M_{0i}}\tilde{x}_{2i}^2}{0.5\overline{M_{0i}}}\right)^{\frac{1}{2}} + \varepsilon_{0i}\tilde{\gamma}_{2i}\hat{\gamma}_{2i} - \\ &\quad \left(\frac{\varepsilon_{0i}(2h_i-1)}{2h_i}\tilde{\gamma}_{2i}^2\right)^{\frac{1}{2}} + \left(\frac{\varepsilon_{0i}(2h_i-1)}{2h_i}\tilde{\gamma}_{2i}^2\right)^{\frac{1}{2}} \\ &\le -\delta_i\left[\left(\frac{1}{2}\overline{M_{0i}}\tilde{x}_{2i}^2\right)^{\frac{1}{2}} + \left(\frac{1}{2}\tilde{x}_{1i}^2\right)^{\frac{1}{2}} + \left(\frac{1}{2p_{0i}}\tilde{\gamma}_{2i}^2\right)^{\frac{1}{2}}\right] \\ &\quad + \left(\frac{\varepsilon_{0i}(2h_i-1)}{2h_i}\tilde{\gamma}_{2i}^2\right)^{\frac{1}{2}} + \varepsilon_{0i}\tilde{\gamma}_{2i}\hat{\gamma}_{2i}\end{aligned} \tag{30}$$

where $h_i \ge 0.5$, $\delta_i = \frac{\varepsilon_{2i}}{\left(0.5\overline{M_{0i}}\right)^{0.5}}$, and $p_{0i} = \frac{h_i\delta_i^2}{\varepsilon_{0i}(2h_i-1)}$.

According to Lemma 2, inequality (30) becomes:

$$\dot{V}_{2i} \le -\delta_i V_{2i}^{\frac{1}{2}} + \left(\frac{\varepsilon_{0i}(2h_i-1)}{2h_i}\tilde{\gamma}_{2i}^2\right)^{\frac{1}{2}} + \varepsilon_{0i}\tilde{\gamma}_{2i}\hat{\gamma}_{2i} \tag{31}$$

Here we will apply some useful tricks from [30] to (31). According to Lemma 1, if $(\varepsilon_{0i}(2h_i-1)/2h_i)\tilde{\gamma}_{2i}^2 > 1$, we have:

$$\begin{aligned}&\left(\frac{\varepsilon_{0i}(2h_i-1)}{2h_i}\tilde{\gamma}_{2i}^2\right)^{\frac{1}{2}} + \varepsilon_{0i}\tilde{\gamma}_{2i}\hat{\gamma}_{2i} \\ &< \left(\frac{\varepsilon_{0i}(2h_i-1)}{2h_i}\tilde{\gamma}_{2i}^2\right) + \varepsilon_{0i}\tilde{\gamma}_{2i}\hat{\gamma}_{2i} \le \frac{\varepsilon_{0i}h_i}{2}\gamma_{2i}^2\end{aligned} \tag{32}$$

If $(\varepsilon_{0i}(2h_i-1)/2h_i)\tilde{\gamma}_{2i}^2 \le 1$, we have:

$$\begin{aligned}&\left(\frac{\varepsilon_{0i}(2h_i-1)}{2h_i}\tilde{\gamma}_{2i}^2\right)^{\frac{1}{2}}\Bigg|_{\frac{\varepsilon_{0i}(2h_i-1)}{2h_i}\tilde{\gamma}_{2i}^2\le 1} \\ &< \left(\frac{\varepsilon_{0i}(2h_i-1)}{2h_i}\tilde{\gamma}_{2i}^2\right)^{\frac{1}{2}}\Bigg|_{\frac{\varepsilon_{0i}(2h_i-1)}{2h_i}\tilde{\gamma}_{2i}^2> 1}\end{aligned} \tag{33}$$

Thus, combining (32) and (33) yields:

$$\left(\frac{\varepsilon_{0i}(2h_i-1)}{2h_i}\tilde{\gamma}_{2i}^2\right)^{\frac{1}{2}}+\varepsilon_{0i}\tilde{\gamma}_{2i}\hat{\gamma}_{2i}\le\frac{\varepsilon_{0i}h_i}{2}\gamma_{2i}^2 \tag{34}$$

Therefore, (31) can be rewritten as:

$$\dot{V}_{2i}\le-\delta_i V_{2i}^{\frac{1}{2}}+\frac{\varepsilon_{0i}h_i}{2}\gamma_{2i}^2 \tag{35}$$

Then, according to Lemma 3, $\tilde{x}_{2i}$ will converge to the field (20) in finite time $t_{2i}\le t_{1i}+\frac{2V(x_0)^{\frac{1}{2}}}{\delta_i\theta_{0i}}$.□

3.2 Multivariable output feedback ANTSMC design

Using the proposed ASMO, position and velocity states x_1, x_2 are reconstructed in finite time which can be used to design ANTSMC.

The dynamic equation of the observer will be rewritten in the body-fixed frame for design simplification as:

$$\begin{aligned}\dot{\hat{\eta}}&=J(\eta)\hat{v}+\gamma_1\mathrm{sgn}(\tilde{\eta})\\ M_0\dot{\hat{v}}&=J^T(\eta)\hat{\gamma}_2\mathrm{sgn}(J(\eta)\bar{v}-J(\eta)\hat{v})\\ &\quad-C_0(\hat{v})\hat{v}-D_0(\hat{v})\hat{v}-g_0(\eta)+\tau\\ \dot{\hat{\gamma}}_2&=p_0\left(-\varepsilon_0\hat{\gamma}_2+|J(\eta)\bar{v}-J(\eta)\hat{v}|\right)\end{aligned} \tag{36}$$

where $J(\eta)\bar{v}=J(\eta)\hat{v}+\left(\gamma_1\mathrm{sgn}(\tilde{\eta})\right)_{eq}$.

Define the estimated tracking errors as:

$$\hat{e}_1=\hat{\eta}-\eta_d,\quad \hat{e}_2=J(\eta)\hat{v}-\dot{\eta}_d \tag{37}$$

Therefore, the estimated tracking error dynamic equation can be written as:

$$\begin{aligned}\dot{\hat{e}}_1&=\hat{e}_2+\gamma_1\mathrm{sgn}(\tilde{\eta})\\ \dot{\hat{e}}_2&=J(\eta)M_0^{-1}\left(J^T(\eta)\hat{\gamma}_2\mathrm{sgn}(J(\eta)\bar{v}-J(\eta)\hat{v})\right.\\ &\quad\left.-C_0(\hat{v})\hat{v}-D_0(\hat{v})\hat{v}-g_0(\eta)+\tau\right)+\dot{J(\eta)}\hat{v}-\ddot{\eta}_d\end{aligned} \tag{38}$$

The nonsingular TSM surface using the estimated system states can be designed as [8,26]:

$$\hat{s}=\hat{e}_1+\beta sig(\hat{e}_2)^{\alpha} \tag{39}$$

where $\beta=diag(\beta_1,\cdots,\beta_4)$, and $\beta_i>0$. $1<\alpha_i=g_i/h_i<2, g_i, h_i$ are odd numbers.

The reaching law is defined as:

$$\dot{\hat{s}}=-diag\left(|\hat{e}_2|^{\alpha-1}\right)\left[k_1\hat{s}+k_2sig(\hat{s})^{\phi}\right] \tag{40}$$

where $0<\phi_i=m_i/n_i<1$, and m_i, n_i are odd positive numbers. $k_1=diag(k_{11},\cdots,k_{14}), k_{1i}\in\mathbb{R}^+, k_2=diag(k_{21},\cdots,k_{24}), k_{2i}\in\mathbb{R}^+$.

Then, design the output feedback ANTSMC as:

$$\begin{aligned}\tau&=\tau_1+\tau_2+\tau_3\\ \tau_1&=M_0J^{-1}(\eta)\left(\ddot{\eta}_d-\dot{J(\eta)}\hat{v}\right)\\ &\quad+C_0(\hat{v})\hat{v}+D_0(\hat{v})\hat{v}+g_0(\eta)\\ \tau_2&=-M_0J^{-1}(\eta)\beta^{-1}\alpha^{-1}\left[k_1\hat{s}\right.\\ &\quad\left.+k_2sig(\hat{s})^{\phi}+sig(\hat{e}_2)^{2-\alpha}\right]\\ \tau_3&=-M_0J^{-1}(\eta)\hat{K}_l\mathrm{sgn}(\hat{s})\\ \dot{\hat{K}}_l&=p\left[-\varepsilon\hat{K}_l+|\hat{s}|\right]\end{aligned} \tag{41}$$

where $p=diag(p_1,\cdots,p_4), p_i\in\mathbb{R}^+, \varepsilon=diag(\varepsilon_1,\cdots,\varepsilon_4)$, $\varepsilon_i\in\mathbb{R}^+$

Theorem 2. Consider an estimated tracking error dynamic equation (38) subjected to the output feedback ANTSMC control law (41). The estimated error $\hat{e}_1, \hat{e}_2$ will converge to the following field (42) in finite time,

$$|\hat{e}_{1i}|<\Omega_{1i}=2\Xi_i,\quad |\hat{e}_{2i}|\le\Omega_{2i} \tag{42}$$

where $\Xi_i=\min\left[\Gamma_i^{\frac{1}{2}},\Gamma_i^{\frac{1}{\phi_i+1}}\right], \Gamma_i=\frac{\varepsilon_i h_i\alpha_i\beta_i K_{li}^2}{2(1-\theta_{1i})k_{2i}}$ and $\Omega_{2i}=\left|\beta_i^{-1}\Xi_i\right|^{1/\alpha_i}$. The tracking error e_1, e_2 will converge to the following field (43) in finite time according to Theorem 1.

$$|e_{1i}|<\Omega_{1i}=2\Xi_i,\quad |e_{2i}|\le\Omega_{2i}+\Delta_i \tag{43}$$

where $e_{1i}=(\eta_i-\eta_d)_i, e_{2i}=\left(J(\eta)v-\dot{\eta}_d\right)_i$.

Proof. Define:

$$\tilde{K}_{li}=K_{li}-\hat{K}_{li},\quad \bar{k}_i=\left(\beta\alpha|\hat{e}_2|^{\alpha-1}\right)_i \tag{44}$$

where $K_{l1}>0, \bar{k}_i\ge 0$.

Choosing a Lyapunov candidate for the estimation error dynamic equation (38) as:

$$V_{3i}=\frac{1}{2}\hat{s}_i^2+\frac{\bar{k}_i}{2p_i}\tilde{K}_{li}^2 \tag{45}$$

Differentiating V_{3i} with respect to time along (38) yields:

$$\begin{aligned}\dot{V}_{3i}&=\hat{s}_i\dot{\hat{s}}_i-\bar{k}_i\tilde{K}_{li}\left(-\varepsilon\hat{K}_l+|\hat{s}|\right)_i\\ &=\hat{s}_i\left(\dot{\hat{e}}_1+\beta\alpha|\hat{e}_2|^{\alpha-1}\dot{\hat{e}}_2\right)_i-\bar{k}_i\tilde{K}_{li}\left(-\varepsilon\hat{K}_l+|\hat{s}|\right)_i\\ &=\hat{s}_i\left(\hat{e}_2+\gamma_1\mathrm{sgn}(\tilde{\eta})+\beta\alpha|\hat{e}_2|^{\alpha-1}\left[\dot{J(\eta)}\hat{v}-\ddot{\eta}_d\right.\right.\\ &\quad\left.\left.+J(\eta)M_0^{-1}\left(J^T(\eta)\hat{\gamma}_2\mathrm{sgn}(\bar{v})-H(\eta,\hat{v})+\tau\right)\right]\right)_i\\ &\quad-\bar{k}_i\tilde{K}_{li}\left(-\varepsilon\hat{K}_l+|\hat{s}|\right)_i\end{aligned} \tag{46}$$

where $\tilde{v} = J(\eta)\bar{v} - J(\eta)\hat{v}$, $H(\eta, \hat{v}) = C_0(\hat{v})\hat{v} + D_0(\hat{v})\hat{v} + g_0(\eta)$

Substituting control law (41) into (46) yields:

$$\begin{aligned}\dot{V}_{3i} &= -\hat{s}_i\left[\vec{k}_1\hat{s} + \vec{k}_2 sig(\hat{s})^{\phi}\right]_i + \gamma_{1i}\hat{s}_i \mathrm{sgn}(\tilde{\eta}_i) \\ &\quad + \bar{k}_i(\varphi(\bullet)\mathrm{sgn}(\tilde{v}))_i\hat{\gamma}_{2i}\hat{s}_i - \bar{k}_i K_{li}|\hat{s}|_i + \varepsilon_i\bar{k}_i\tilde{K}_{li}\hat{K}_{1i} \\ &\le -|\hat{s}_i|\left(\bar{k}K_l - \bar{k}\varphi(\bullet)\hat{\gamma}_2 - \bar{k}_1\gamma_1\right)_i \\ &\quad - \hat{s}_i\left[\vec{k}_1\hat{s} + \vec{k}_2 sig(\hat{s})^{\phi}\right]_i + \varepsilon_i\bar{k}_i\tilde{K}_{li}\hat{K}_{1i}\end{aligned} \tag{47}$$

where $\vec{k}_1 = |\hat{e}_2|^{\alpha-1}k_1, \vec{k}_2 = |\hat{e}_2|^{\alpha-1}k_2, \varphi(\bullet) = [J(\eta)M_0J(\eta)^T]$

Choosing an appropriately large K_{li} to make $\left(\bar{k}K_l - \bar{k}\varphi(\bullet)\hat{\gamma}_2 - \bar{k}_1\gamma_1\right)_i > 0$ yields:

$$\dot{V}_{3i} \le -\hat{s}_i\left[\vec{k}_1\hat{s} + \vec{k}_2 sig(\hat{s})^{\phi}\right]_i + \varepsilon_i\bar{k}_i\tilde{K}_{li}\hat{K}_{1i} \tag{48}$$

Therefore, the following two inequalities can be obtained from (48):

$$\dot{V}_{3i} \le -\vec{k}_{2i}|\hat{s}_i|^{\phi_i+1} + \varepsilon_i\bar{k}_i\tilde{K}_{li}\hat{K}_{1i} \tag{49}$$

$$\dot{V}_{3i} \le -\vec{k}_{1i}|\hat{s}_i|^2 + \varepsilon_i\bar{k}_i\tilde{K}_{li}\hat{K}_{1i} \tag{50}$$

For (49), noticing Lemma 1, we have:

$$\varepsilon_i\bar{k}_i\tilde{K}_{li}\hat{K}_{1i} \le \frac{-\varepsilon_i\bar{k}_i(2h_i-1)}{2h_i}\tilde{K}_{li}^2 + \frac{\varepsilon_i\bar{k}_ih_i}{2}K_{li}^2 \tag{51}$$

where $h_i > 0.5$ is a positive number.

Therefore, inequality (49) becomes:

$$\begin{aligned}\dot{V}_{3i} &\le -2^{\frac{\phi_i+1}{2}}\vec{k}_{2i}\left(\frac{1}{2}\hat{s}_i^2\right)^{\frac{\phi_i+1}{2}} - \left(\frac{\varepsilon_i\bar{k}_i(2h_i-1)}{2h_i}\tilde{K}_{li}^2\right)^{\frac{\phi_i+1}{2}} \\ &\quad + \left(\frac{\varepsilon_i\bar{k}_i(2h_i-1)}{2h_i}\tilde{K}_{li}^2\right)^{\frac{\phi_i+1}{2}} + \varepsilon_i\bar{k}_i\tilde{K}_{li}\hat{K}_{1i} \\ &\le -\chi_i\left(\left(\frac{1}{2}\hat{s}_i^2\right)^{\frac{\phi_i+1}{2}} + \left(\frac{\bar{k}_i}{2p_{li}}\tilde{K}_{li}^2\right)^{\frac{\phi_i+1}{2}}\right) \\ &\quad + \frac{\varepsilon_i\bar{k}_ih_i}{2}K_{li}^2\end{aligned} \tag{52}$$

where: $\chi_i = 2^{\frac{\phi_i+1}{2}}\vec{k}_{2i}, p_{1i} = \frac{h_i\chi_i^{2/(\phi_i+1)}}{\varepsilon_i(2h_i-1)}$.

Take Lemma 2 and $\frac{1}{2} < \frac{\phi_i+1}{2} < 1$ into consideration; then (52) becomes:

$$\begin{aligned}\dot{V}_{3i} &\le -\chi_i\left(\frac{1}{2}\hat{s}_i^2 + \frac{\bar{k}_i}{2p_{li}}\tilde{K}_{li}^2\right)^{\frac{\phi_i+1}{2}} + \frac{\varepsilon_i\bar{k}_ih_i}{2}K_{li}^2 \\ &\le -\chi_i V_{3i}^{\frac{\phi_i+1}{2}} + \frac{\varepsilon_i\bar{k}_ih_i}{2}K_{li}^2\end{aligned} \tag{53}$$

Therefore, according to Lemma 3, the trajectory of (49) will be forced to the following field in finite time:

$$|\hat{s}_i| \le \left(\frac{\varepsilon_ih_i\alpha_i\beta_iK_{li}^2}{2(1-\theta_{1i})k_{2i}}\right)^{\frac{1}{\phi_i+1}} \tag{54}$$

Applying the similar analysis procedure to (50) yields:

$$|\hat{s}_i| \le \left(\frac{\varepsilon_ih_i\alpha_i\beta_iK_{li}^2}{2(1-\theta_{1i})k_{2i}}\right)^{\frac{1}{2}} \tag{55}$$

Thus, combining (54) and (55), the tracking trajectory of the closed-loop system will be forced into the following field in finite time.

$$\Xi_i = \min\left[\Gamma_i^{\frac{1}{2}}, \Gamma_i^{\frac{1}{\phi_i+1}}\right], \quad \Gamma_i = \frac{\varepsilon_ih_i\alpha_i\beta_iK_{li}^2}{2(1-\theta_{1i})k_{2i}} \tag{56}$$

Note that, in (47), $\hat{e}_{2i} = 0$ may hinder the reachability of TSM (39). Nevertheless, it will be shown that $\hat{e}_{2i} = 0$ is not an attractor in the reaching phase. Substituting control law (41) into (38) yields:

$$\begin{aligned}\dot{\hat{e}}_i &= \left(\varphi(\bullet)\hat{\gamma}_2\mathrm{sgn}(\tilde{v})\right)_i - \beta_i^{-1}\alpha_i^{-1}\left[k_{1i}\hat{s}_i + \right. \\ &\quad \left. k_{2i}sig(\hat{s}_i)^{\phi_i} + sig(\hat{e}_{2i})^{2-\alpha_i}\right] - \hat{K}_{li}\mathrm{sgn}(\hat{s}_i)\end{aligned} \tag{57}$$

In the case of $\hat{e}_{2i} = 0$ and $\hat{s}_i \ne 0$, we have $\dot{\hat{e}}_i \ne 0$. Therefore, the finite-time reachability of TSM (39) is ensured [8].

Combining (39) and (56), we have:

$$\hat{s}_i = \hat{e}_{1i} + \beta_i sig(\hat{e}_{2i})^{\alpha_i} \le \Xi_i \tag{58}$$

Equation (58) can be further rewritten as:

$$0 = \hat{e}_{1i} + \left(\beta_i - \hat{s}_i sig(\hat{e}_{2i})^{-\alpha_i}\right) sig(\hat{e}_{2i})^{\alpha_i} \tag{59}$$

When $\left(\beta_i - \hat{s}_i sig(\hat{e}_{2i})^{-\alpha_i}\right) > 0$, (59) still keeps the same form with TSM (39), therefore $\hat{e}_{2i}$ will converge to the following field in finite time:

$$|\hat{e}_{2i}| \le \left|\beta_i^{-1}\hat{s}_i\right|^{1/\alpha_i} \le \left(\beta_i^{-1}\Xi_i\right)^{1/\alpha_i} = \Omega_{2i} \tag{60}$$

Combining (59) and (60), we have:

$$\begin{aligned}\left|\hat{e}_{1i}\right| &= \left|\hat{s}_i - \beta_i sig\left(\hat{e}_{2i}\right)^{\alpha_i}\right| \\ &\leq \left|\beta_i sig\left(\hat{e}_{2i}\right)^{\alpha_i}\right| + \left|\hat{s}_i\right| \leq 2\Xi_i\end{aligned} \tag{61}$$

Therefore, the estimated error $\hat{e}_i, \hat{e}_2$ will converge to the field (42) in finite time. And according to Theorem 1, the tracking error e_1, e_2 will converge to the field (43) in finite time.

Remark 2. Upper bound information of the lumped uncertainties is needed to choose γ_{2i} and K_{li} . But it should be noted that, γ_{2i} and K_{li} are only used for calculating corresponding errors and analyzing stability of the system. They are not directly used in ASMO (16) and ANTSMC (41).

Remark 3. Compared with the methods presented in [26] and [27], the new proposed one in this article does not need any information of the lumped uncertainties, which is almost impossible to obtain in many practical applications. Thus, γ_{2i} and K_{li} can be decreased greatly due to the adoption of adaptive law leading to relatively smooth velocity estimation and control effort.

Remark 4. From Theorem 1 and Theorem 2, it seems that the tracking performance of the proposed observer-controller system is not as good as the one from [26] or [27]. It should be noted that, the observer-controller systems presented in [26] and [27] may not be realizable in many applications due to their requirement of the bound information of lumped uncertainties. Even when the control systems can be realized by using relatively large γ_2 and K_l, the chattering will also destroy the control performance. In short, the proposed ANTSMC based on equivalent output injection ASMO is more realizable in practical applications.

IV. SIMULATION ANALYSES

To illustrate the effectiveness of the proposed method (ANTSMC), comparative numerical simulations are performed using the model of a small ROV called POLARIS shown in Fig. 1. It is compared with the control methods from [26] and [27], which require the bound information of lumped uncertainties and use fixed control parameters. They are indicated as output feedback nonsingular terminal sliding mode control (NTSMC) and output feedback sliding mode control (SMC) in the following text.

The SMO used in [26,27] can be extended for the MIMO systems using the same design procedure presented in Section 3.1:

$$\begin{aligned}\dot{\hat{\eta}} &= J(\eta)\hat{v} + \gamma_1 \mathrm{sgn}\left(\tilde{\eta}\right) \\ M_0\dot{\hat{v}} &= J^T(\eta)\gamma_2 \mathrm{sgn}\left(J(\eta)\bar{v} - J(\eta)\hat{v}\right) \\ &\quad - C_0\left(\hat{v}\right)\hat{v} - D_0\left(\hat{v}\right)\hat{v} - g_0(\eta) + \tau\end{aligned} \tag{62}$$

The NTSMC used in [26] can also be extended for the MIMO systems with the same design procedure presented in Section 3.2:

$$\begin{aligned}\tau &= \tau_1 + \tau_2 + \tau_3 \\ \tau_1 &= M_0 J^{-1}(\eta)\left(\ddot{\eta}_d - \dot{J(\eta)}\hat{v}\right) \\ &\quad + C_0\left(\hat{v}\right)\hat{v} + D_0\left(\hat{v}\right)\hat{v} + g_0(\eta) \\ \tau_2 &= -M_0 J^{-1}(\eta)\beta^{-1}\alpha^{-1} sig\left(\hat{e}_2\right)^{2-\alpha} \\ \tau_3 &= -M_0 J^{-1}(\eta) K_l \mathrm{sgn}\left(\hat{s}\right)\end{aligned} \tag{63}$$

Additionally, the SMC used in [27] can be extended for the MIMO systems by changing the parameter α in (39) and (63) to 1.

Table I. Nominal physical parameters of POLARIS ROV.

Parameters	Value	Parameters	Value
m/kg	5.1	X_u/(kg/s)	-11.2
W/N	50	Y_v/(kg/s)	-13.5
B/N	50.4	Z_w/(kg/s)	-16.5
Z_B/m	-0.05	N_r/(kg · m^2/(s · rad))	-9.6
I_x/ (kg · m^2)	0.2	$X_{u\|u\|}$/(kg/m)	-3.2
I_y/ (kg · m^2)	0.6	$Y_{v\|v\|}$/(kg/m)	-2.7
I_z/ (kg · m^2)	0.9	$Z_{w\|w\|}$/(kg/m)	-3.5
$X_{\dot{u}}$/kg	-3.3	$N_{r\|r\|}$/ (kg · m^2/rad^2)	-1.3
$Y_{\dot{v}}$/kg	-4.3	τ_{fmax}/N	1.6
$Z_{\dot{w}}$/kg	-6.4	τ_{bmax}/N	-3.2
$N_{\dot{r}}$/ (kg · m^2)	-1.8		

Table II. Control parameters.

ANTSMC	$\gamma_{1i} = 8$	$p_{0i} = 9$	$p_i = 9$
	$\varepsilon_{0i} = 0.05$	$\varepsilon_i = 0.05$	$\beta_i = 1$
	$\alpha_i = 9/7$	$k_{1i} = 1$	$k_{2i} = 1$
	$\phi_i = 3/7$	$\hat{\gamma}_{2i}(0) = 0$	$\hat{K}_{li}(0) = 0$
NTSMC	$\gamma_{1i} = 8$	$\gamma_{2i} = 3$	$\beta_i = 1$
	$\alpha_i = 9/7$	$K_{li} = 3$	
SMC	$\gamma_{1i} = 8$	$\gamma_{2i} = 3$	$\beta_i = 1$
	$\alpha_i = 1$	$K_{li} = 3$	

$$\begin{aligned}\tau &= \tau_1 + \tau_2 + \tau_3\\ \tau_1 &= M_0 J^{-1}(\eta)\left(\ddot{\eta}_d - \dot{J}(\eta)\hat{v}\right)\\ &\quad + C_0(\hat{v})\hat{v} + D_0(\hat{v})\hat{v} + g_0(\eta)\\ \tau_2 &= -M_0 J^{-1}(\eta)\beta^{-1}\hat{e}_2\\ \tau_3 &= -M_0 J^{-1}(\eta)K_l \mathrm{sgn}(\hat{s})\end{aligned} \tag{64}$$

The nominal physical parameters of POLARIS are listed in Table I. The control parameters of ANTSMC, NTSMC and SMC are listed in Table II.

The initial values for all the three controllers are $\eta_i(0) = -0.2, v_i(0) = 0, \hat{\eta}_i(0) = 0$ and $\hat{v}_i(0) = -0.2$.

To make the comparison fair and persuasive, corresponding control parameters for the three controllers

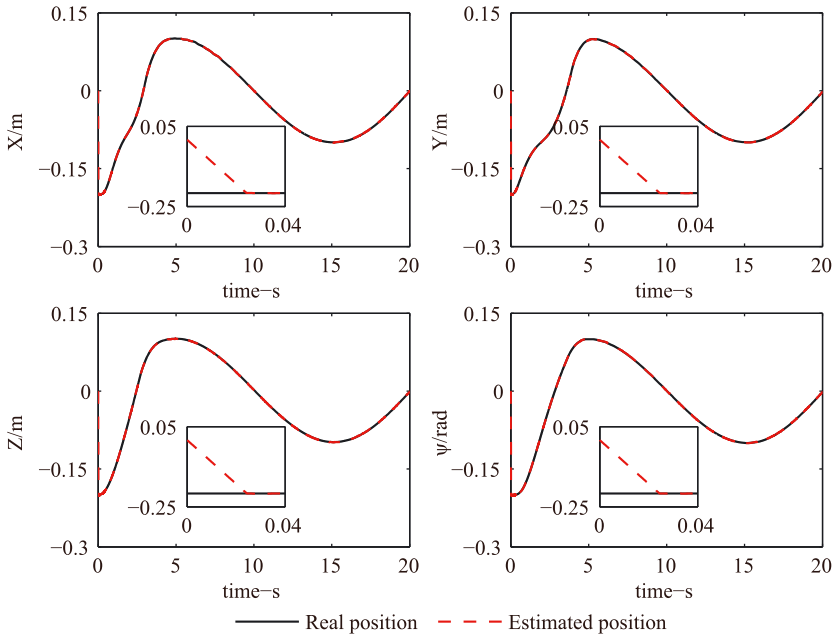

Fig. 3. Real position and estimated position of output feedback ANTSMC.

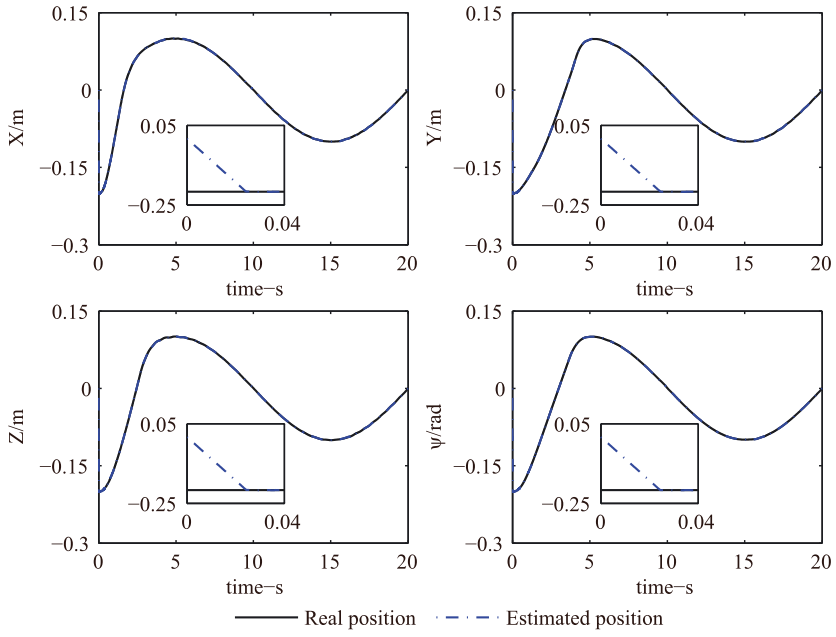

Fig. 4. Real position and estimated position of output feedback NTSMC.

are selected exactly the same as shown in Table II. The dynamics of the propellers are also taken into account. We treat the propellers as one-order inertial systems with a time constant of 0.2 seconds. The simulation is implemented in SIMULINK using a fixed-step fourth-order Runge-Kutta solver with a sample period of $T = 0.0002$ s. The desired trajectory is chosen as $\eta_d = 0.1sin(0.1\pi t)$, and the external disturbance is $d = 0.1sin(0.2\pi t)$. To illustrate the robustness of the controllers for parametric uncertainties, the physical parameters used in the observers and controllers are 20% smaller than those used in ROV's model.

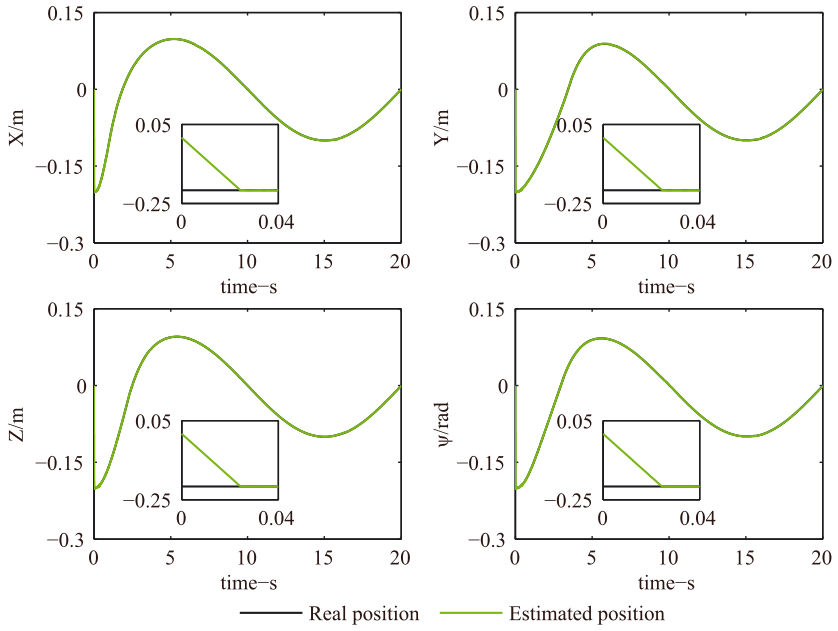

Fig. 5. Real position and estimated position of output feedback SMC.

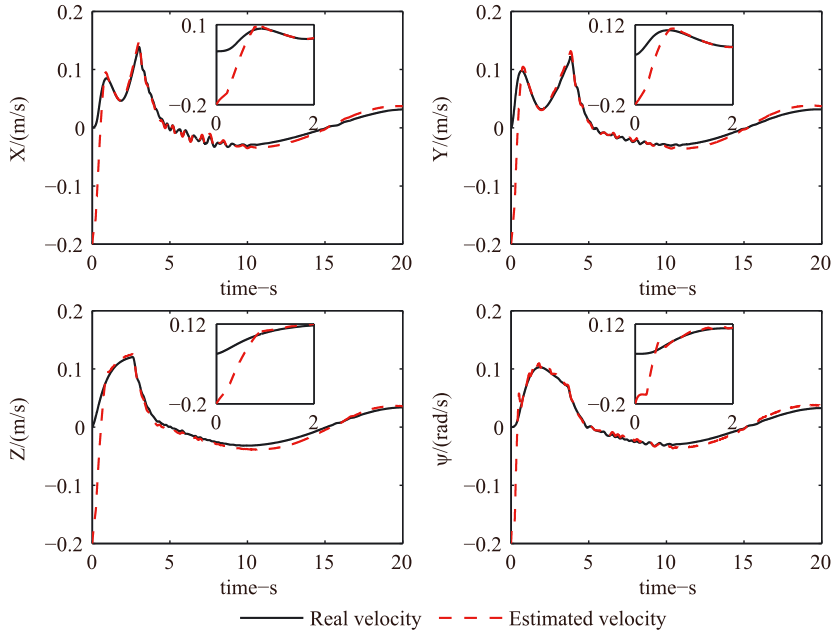

Fig. 6. Real velocity and estimated velocity of output feedback ANTSMC.

Figs 3–8 show the estimated positions/velocities using the proposed ASMO (16) and SMO (62) compared with their real values for all the three observer-controller systems. It can be seen clearly that the estimated positions and velocities converge to their real values in finite time of about 0.02 seconds and 0.8 seconds using both observers in the presence of disturbances and parametric uncertainties. Furthermore, the proposed ASMO (16)

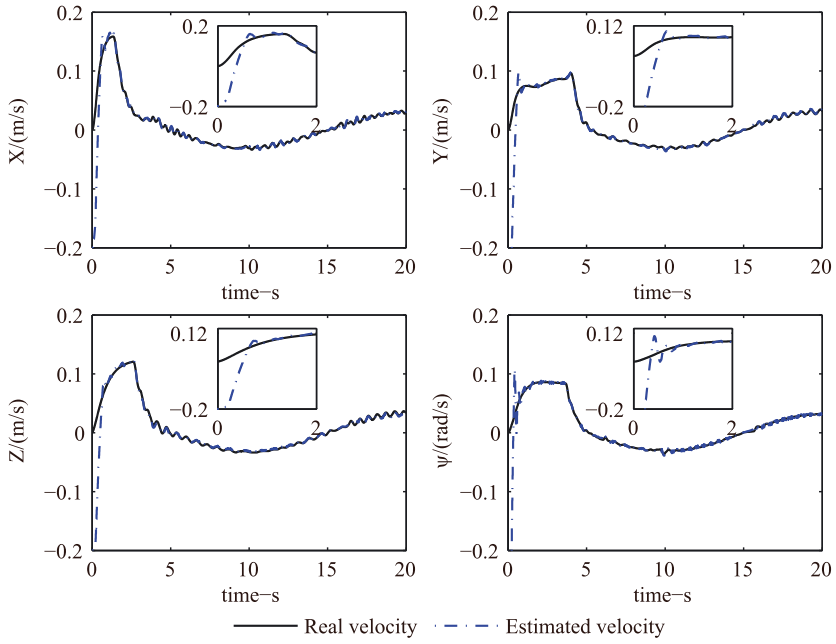

Fig. 7. Real velocity and estimated velocity of output feedback NTSMC.

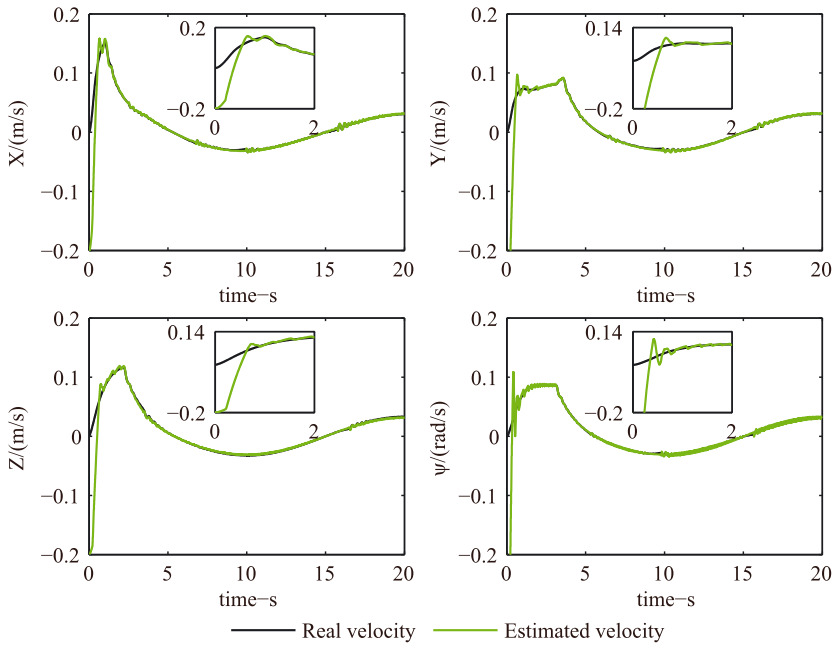

Fig. 8. Real velocity and estimated velocity of output feedback SMC.

can provide relatively more smooth estimated velocities compared with SMO (62) especially in the initial stage. As the bound information of the lumped uncertainties is almost impossible to obtain in most practical applications, a large observer parameter γ_2 is required to ensure the stability of the observer which, however, may lead to severe chattering in the estimation of velocities. Since the estimated velocities are directly used in the controllers, a relatively smooth estimated velocity will effectively reduce the chattering of the control effort.

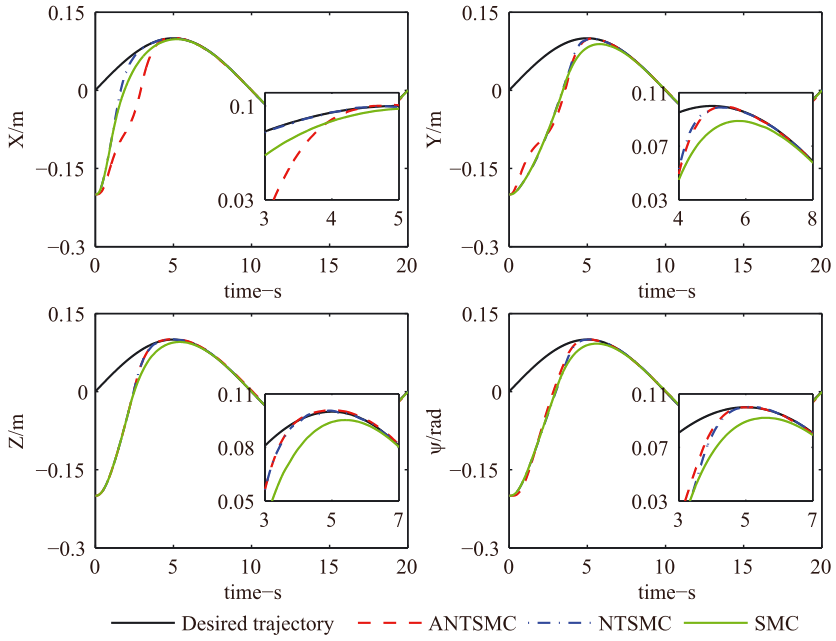

Fig. 9. Tracking performance of output feedback ANTSMC, NTSMC and SMC.

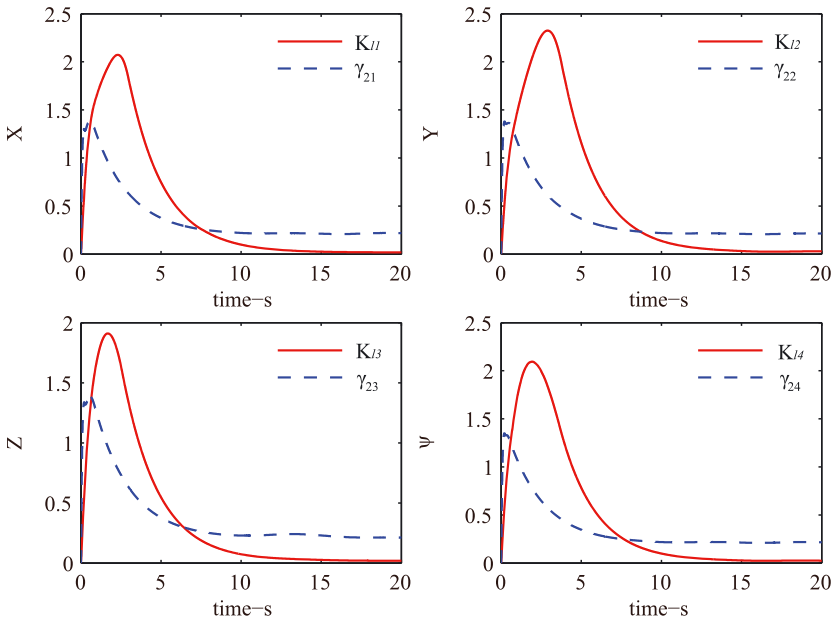

Fig. 10. Estimated parameters of ANTSMC.

Fig. 9 shows the tracking performance using output feedback ANTSMC, NTSMC and SMC. It can be seen that all the three controllers have great robustness against parametric uncertainties and external disturbances. Meanwhile, ANTSMC can achieve almost the same convergence speed as NTSMC, and both of them can

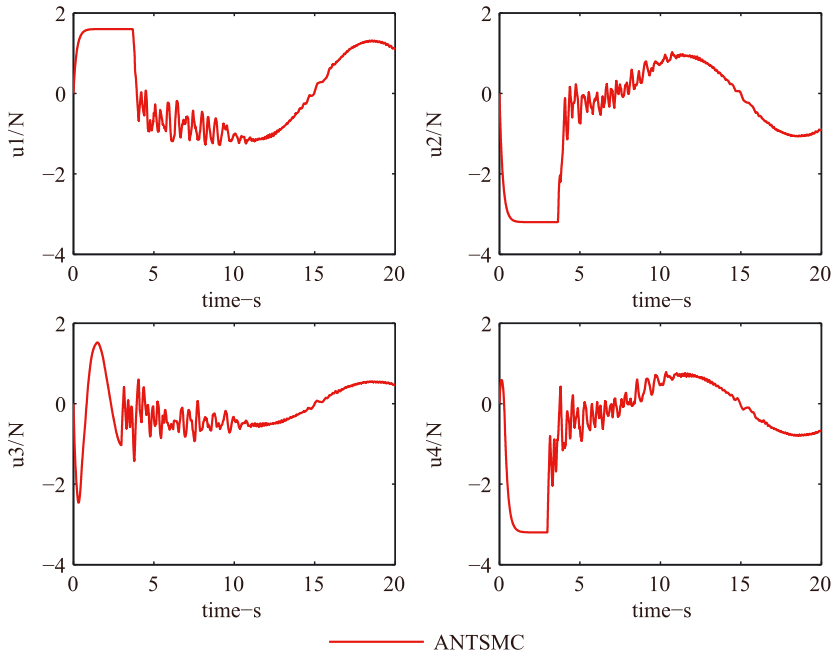

Fig. 11. Control inputs of output feedback ANTSMC(u1-u4).

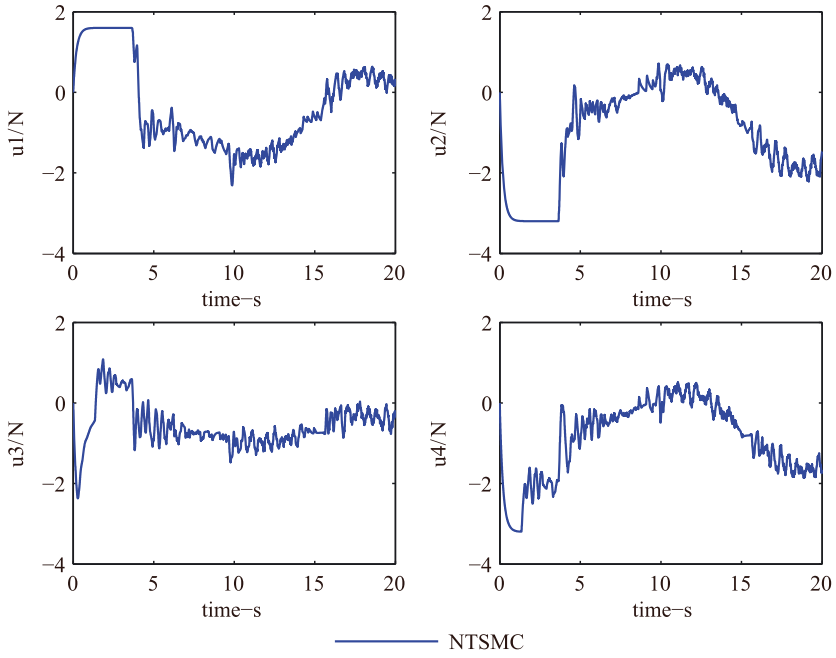

Fig. 12. Control inputs of output feedback NTSMC(u1-u4).

provide a faster convergence speed than the SMC method which illustrates the advantage of TSM over the traditional SM.

Fig. 10 shows the tendency of the adaptive parameters $\hat{K}_l$ and $\hat{\gamma}_2$. It is clear that parameter $\hat{K}_l$ and $\hat{\gamma}_2$ converge to constants with initial values of zero. It should be noted that the estimation error $\tilde{K}_l$ and $\tilde{\gamma}_2$ may not converge to zero since the derivation of (27) and (45) are not strictly negative.

Figs 11–14 show the control efforts of output feedback ANTSMC, NTSMC and SMC. All the three methods have chattering in the beginning phase. But later on, compared with NTSMC and SMC which use fixed gain for the discontinuous term τ_3, ANTSMC can provide

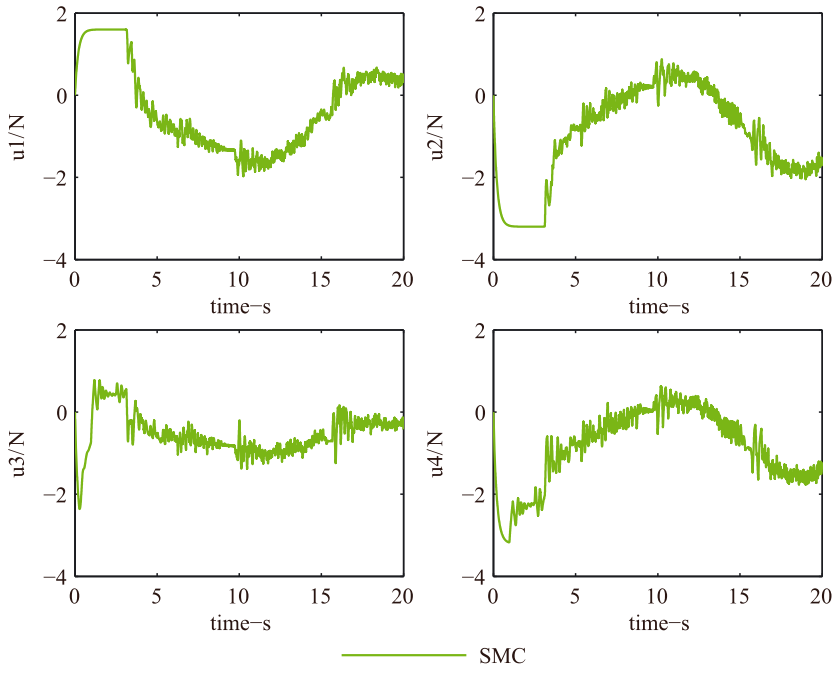

Fig. 13. Control inputs of output feedback SMC(u1-u4).

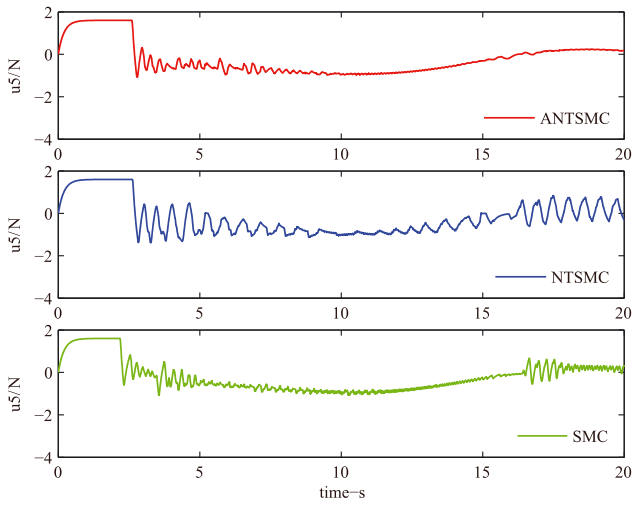

Fig. 14. Control inputs of output feedback ANTSMC, NTSMC and SMC of u5.

with relatively more smooth control efforts benefiting from the adaptive gain for τ_3.

Chattering can be weakened using many technologies. Replacing the signum function with saturation function is a simple and effective way. A saturation function can be expressed as follows:

$$\text{sat}\left(\frac{x}{\Delta}\right) = \begin{cases} x/|x|, & |x| \geq \Delta \\ x/\Delta, & |x| < \Delta \end{cases} \tag{65}$$

Δ is the boundary layer. Then choosing a boundary layer $\Delta_i = 0.02$ for the control laws (41), (63) and (64). The performance of output feedback ANTSMC,

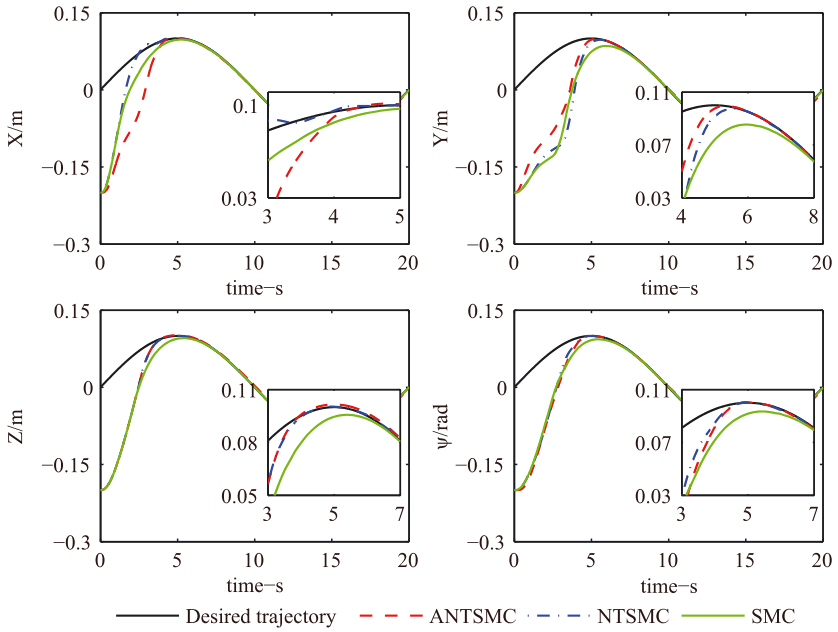

Fig. 15. Tracking performance of output feedback ANTSMC, NTSMC and SMC with boundary layer.

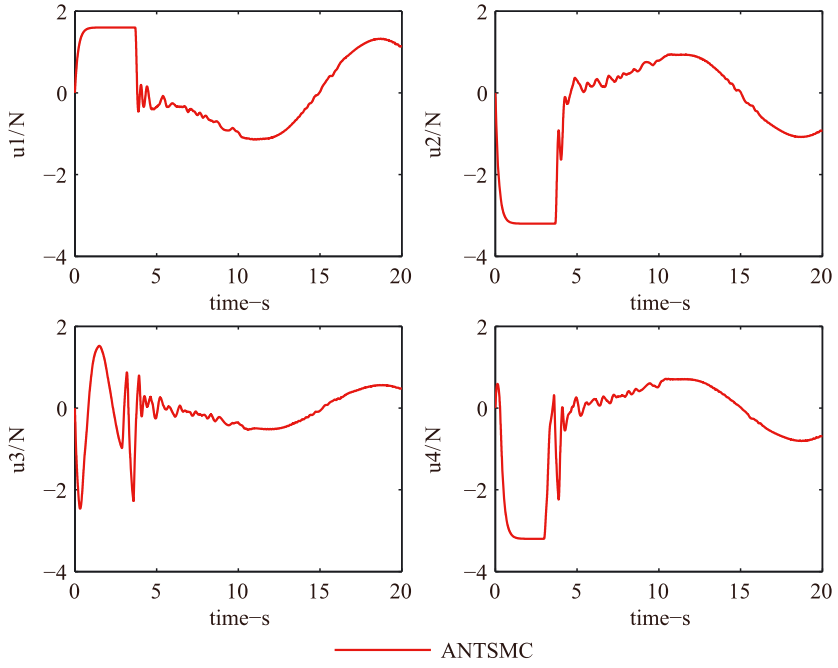

Fig. 16. Control inputs of output feedback ANTSMC with boundary layer (u1-u4).

NTSMC and SMC with boundary layers are given in Figs 15–19.

Fig. 15 shows that such replacements have little impact on the tracking performance of the control systems. Furthermore, comparing Figs 16–19 with Figs 11–14, it can be seen clearly that chattering is weakened effectively for ANTSMC, NTSMC and SMC. Meanwhile, the output feedback ANTSMC can still

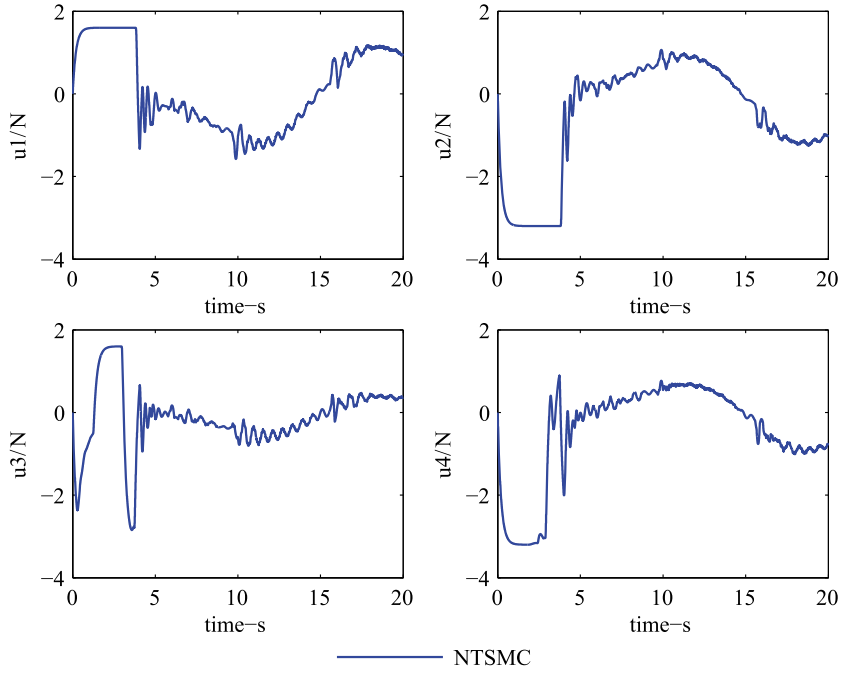

Fig. 17. Control inputs of output feedback NTSMC with boundary layer (u1-u4).

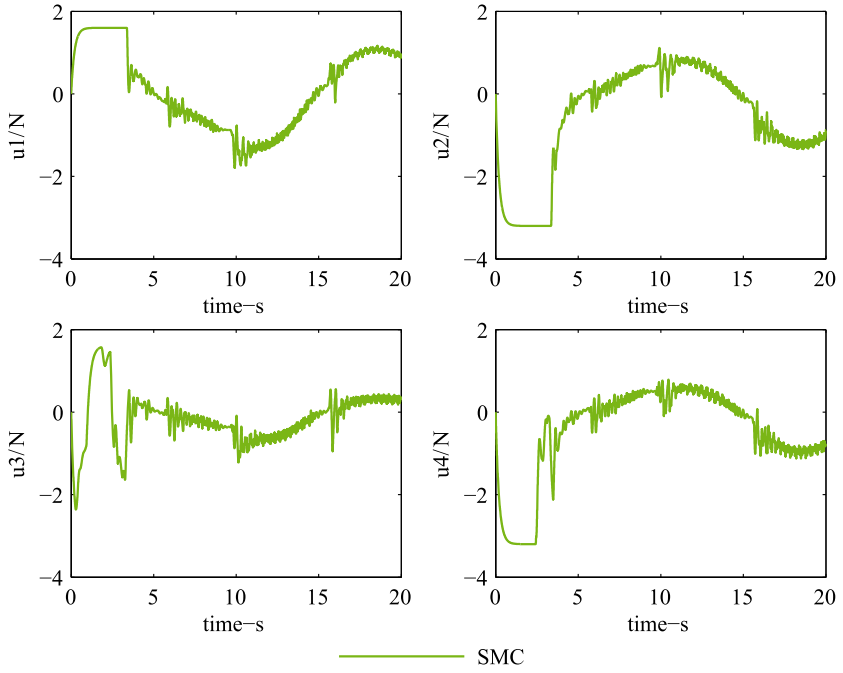

Fig. 18. Control inputs of output feedback SMC with boundary layer (u1-u4).

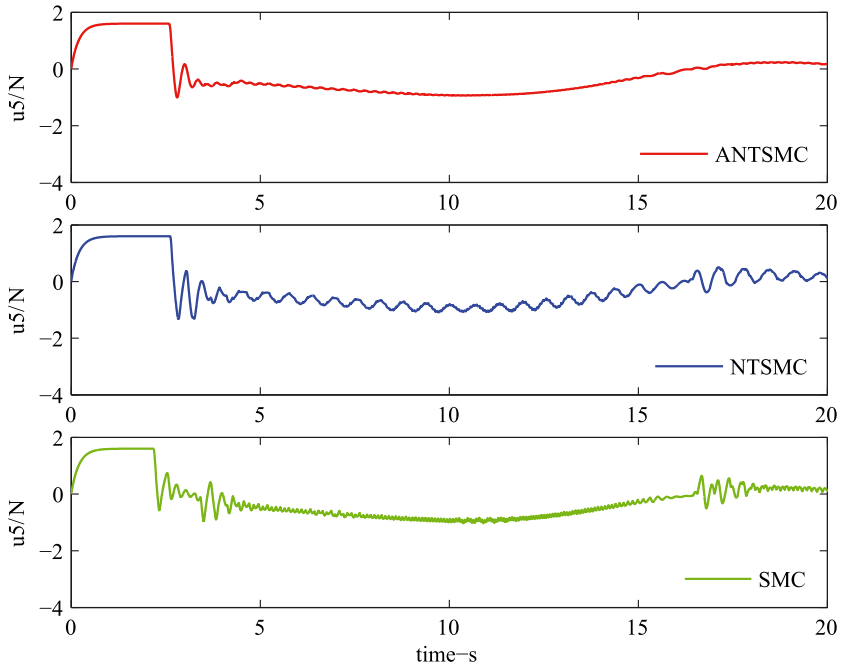

Fig. 19. Control inputs of output feedback ANTSMC, NTSMC and SMC of u5 with boundary layer.

provide with the most smooth control effort among all the three methods benefiting from the adaptive technology.

It should be mentioned that a larger boundary layer may further weaken the chattering which bothers NTSMC and SMC, but it may not be eliminated due to the relatively large fixed system parameters $\hat{K}_l$ and $\hat{\gamma}_2$. Besides, a over large boundary layer may destroy the tracking performance. Therefore, NTSMC and SMC are less suitable than ANTSMC in the physical applications due to the relatively apparent chattering after the adoption of boundary technology.

From all these figures (Figs 3–19), it can be concluded that fixed large parameters for observer-controller systems can provide faster convergence speed and stronger robustness compared with the adaptive ones. However, over large fixed parameters may lead to severe chattering which, in turn, can result in serious damage to the practical systems. Meanwhile due to the lack of bound information of the lumped uncertainties, it is nearly impossible to find suitable fixed parameters for all kinds of applications. This leads to the fact that the NTSMC and SMC from [26] and [27] which use fixed control parameters is not suitable in many applications even with the help of boundary layer technology. Therefore, using adaptive technology to estimate the information of lumped uncertainties is necessary in the view of practical applications.

V. CONCLUSIONS

A multivariable output feedback ANTSMC approach based on equivalent output injection ASMO and ANTSMC method is proposed for the MIMO control systems of ROVs. It guarantees the finite-time convergence of the estimation/tracking errors to bounded small fields. Compared with the output feedback NTSMC/SMC control algorithms from [26] and [27], the new proposed approach does not require bound information of the lumped uncertainties and can provide with relatively more smooth velocity estimation and control effort. Therefore, the new proposed approach is more suitable for physical applications. Stability analysis and numerical simulations are preformed to validate the effectiveness of the proposed approach.

REFERENCES

1. Hoang, N. Q. and E. Kreuzer, "A robust adaptive sliding mode controller for remotely operated vehicles," *Tech. Mech.*, Vol. 3-4, No. 28, pp. 185–193 (2008).
2. Yang, L. and J. Yang, "Nonsingular fast terminal sliding mode control for nonlinear dynamical systems," *Int. J. Robust. Nonlinear Control.*, Vol. 21, No. 16, pp. 1865–1879 (2011).
3. Healy, A. J. and D. Lienard, "Multivariable sliding mode control for autnomous diving and steering

of unmanned underwater vehicles," *IEEE J. Ocean. Eng.*, Vol. 18, No. 3, pp. 327–339 (1993).
4. Zhang, M. and Z. Chu, "Adaptive sliding mode control based on local recurrent neural network for underwater robot," *Ocean. Eng.*, Vol. 45, pp. 56–62 (2012).
5. Li, J., H. Su, Y. Zhang, Z. Wu, and J. Chu, "Chattering free sliding mode control for uncertain discrete time-delay singular systems," *Asian J. Control*, Vol. 15, No. 1, pp. 260–269 (2013).
6. Corradini, M. L., G. Ippoliti, S. Longhi, D. Marchei, and G. Orlando, "A quasi-sliding mode observer-based controller for PMSM drives," *Asian J. Control*, Vol. 15, No. 2, pp. 380–390 (2013).
7. Zhao, D., Y. Wang, L. Liu, and Z. Wang, "Robust fault-tolerant control of launch vehicle via GPI observer and integral sliding mode control," *Asian J. Control*, Vol. 15, No. 2, pp. 614–623 (2013).
8. Yu, S., X. Yu, and B. Shirinzadeh, "Continuous finite-time control for robotic manipulators with terminal sliding mode," *Automatica*, Vol. 41, No. 11, pp. 1957–1964 (2005).
9. Zak, M., "Terminal attractor for addressable memory in neural network," *Phys. Lett. A*, Vol. 133, No. 1/2, pp. 18–22 (1988).
10. Man, Z., A. P. Paplinski, and H. R. Wu, "A robust MIMO terminal sliding mode control for rigid robotic manipulators," *IEEE Trans. Autom. Control*, Vol. 39, No. 12, pp. 2464–2469 (1994).
11. Yu, X. and Z. Man, "Multi-input uncertain linear systems with terminal sliding-mode control," *Automatica*, Vol. 34, No. 3, pp. 389–392 (1998).
12. Feng, Y., X. Yu, and Z. Man, "Non-singular terminal sliding mode control of rigid manipulators," *Automatica*, Vol. 38, No. 12, pp. 2159–2167 (2002).
13. Jin, M., J. Lee, P. H. Chang, and C. Choi, "Practical nonsingular terminal sliding-mode control of robot manipulators for high-accuracy tracking control," *IEEE Trans. Ind. Electron.*, Vol. 56, No. 9, pp. 3593–3601 (2009).
14. Zhao, D. and T. Zou, "A finite-time approach to formation control of multiple mobile robots with terminal sliding mode," *Int. J. Syst. Sci.*, Vol. 43, No. 11, pp. 1998–2014 (2012).
15. Li, H., L. Dou, and Z. Su, "Adaptive nonsingular fast terminal sliding mode control for electromechanical actuator," *Int. J. Syst. Sci.*, Vol. 44, No. 3, pp. 401–415 (2013).
16. Yang, C. C., "Robust adaptive terminal sliding mode synchronized control for a class of non-autonomous chaotic systems," *Asian J. Control*, Vol. 15, No. 6, pp. 1677–1685 (2013).
17. Imsland, L., T. A. Johansen, T. I. Fossen, H. F. Grip, J. C. Kalkkuhl, and A. Suissa, "Vehicle velocity estimation using nonlinear observers," *Automatica*, Vol. 42, No. 12, pp. 2091–2103 (2006).
18. Fossen, T. I. and A. Grovlen, "Nonlinear output feedback control of dynamically positioned ships using vectorial observer backstepping," *IEEE Trans. Control Syst. Technol.*, Vol. 6, No. 1, pp. 121–128 (1998).
19. Ahmadizadeh, S., J. Zarei, and H. R. Karimi, "Robust unknown input observer design for linear uncertain time delay systems with application to fault detection," *Asian J. Control*, Vol. 16, No. 4, pp. 1006–1019 (2014).
20. Soga, T. and N. Otsuka, "Quadratic stabilizability for polytopic uncertain switched linear systems via switched observer," *Asian J. Control*, Vol. 16, No. 4, pp. 1020–1028 (2014).
21. Battilotti, S., "Incremental generalized homogeneity, observer design and semiglobal stabilization," *Asian J. Control*, Vol. 16, No. 2, pp. 498–508 (2014).
22. Anwar, S. and N. Wei, "A nonlinear observer based analytical redundancy for predictive fault tolerant control of a steer-by-wire system," *Asian J. Control*, Vol. 16, No. 2, pp. 321–334 (2014).
23. That, L. T. and Z. Ding, "Adaptive lipschitz observer design for a mammalian model," *Asian J. Control*, Vol. 16, No. 2, pp. 335–344 (2014).
24. Zhou, L., J. She, and S. Zhou, "Design of robust discrete-time observer-based repetitive-control system," *Asian J. Control*, Vol. 16, No. 2, pp. 509–518 (2014).
25. Edwards, C. and C. P. Tan, "A comparison of sliding mode and unknown input observers for fault reconstruction," *Eur. J. Control*, Vol. 12, No. 3, pp. 245–260 (2006).
26. Zhao, D., S. Li, and Q. Zhu, "Output feedback terminal sliding mode control for a class of second order nonlinear systems," *Asian J. Control*, Vol. 15, No. 1, pp. 237–247 (2013).
27. Daly, J. M. and D. W. L. Wang, "Output feedback sliding mode control in the presence of unknown disturbances," *Syst. Control Lett.*, Vol. 58, No. 3, pp. 188–193 (2009).
28. Haskara, I., U. Ozguner, and V. Utkin, "On sliding mode observers via equivalent control approach," *Int. J. Control*, Vol. 71, No. 6, pp. 1051–1067 (1998).
29. Fossen, T. I., *Guidance and Control of Ocean Vehicles*, John Wiley and Sons, New York, NY (1994).
30. Zhu, Z., Y. Xia, and M. Fu, "Attitude stabilization of rigid spacecraft with finite-time convergence," *Int. J. Robust Nonlinear Control*, Vol. 21, No. 6, pp. 686–702 (2011).

31. Barambones, O. and V. Etxebarria, "Energy-based approach to sliding composite adadptive control for rigid robots with finite error convergence time," *Int. J. Control*, Vol. 75, No. 5, pp. 352–359 (2002).
32. Hale, J. K., *Ordinary Differential Equations*, Krieger, Huntington, NJ (1969).

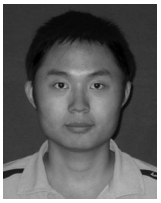

Yaoyao Wang, born in 1989, is currently a Ph.D. candidate at The State Key Laboratory of Fluid Power Transmission and Control, Zhejiang University, China. He received his B.S. degree from Southeast University, Nanjing, China, in 2011. His research interests include robust control and adaptive control of ROV and manipulators.

Linyi Gu, born in 1973, is currently Professor and Ph.D. candidate supervisor at The State Key Laboratory of Fluid Power Transmission and Control, Zhejiang University, China. He received his B.S. degree and Ph.D. degree from Zhejiang University, Hangzhou, China, in 1993 and 1998 respectively. His main research interests include underwater vehicles, switch-mode hydraulics and its application, underwater manipulator and long piston sediment corer.

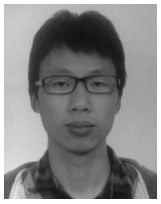

Ming Gao, born in 1987, received his B.S. degree from Huazhong University of Science and Technology, Wuhan, China, in 2011 and M.S. degree from Zhejiang University, Hangzhou, China, in 2014, respectively.

Kangwu Zhu, born in 1983, is with Shanghai Institute of Spaceflight Control Technology, Shanghai, China. He received his B.S. degree from Harbin Institute of Technology, Harbin, China, in 2005, M.S. degree from China Ship Scientific Research Center, Wuxi, China, in 2008, and Ph.D. from Zhejiang University, Hangzhou, China, in 2012. His research interests include sliding mode control and nonlinear system control.